JCTC Journal of Chemical Theory and Computation

Article

pubs.acs.org/JCTC

# Spin Density Distribution in Open-Shell Transition Metal Systems: A Comparative Post-Hartree−Fock, Density Functional Theory, and Quantum Monte Carlo Study of the $CuCl_2$ Molecule

Michel Caffarel,* Emmanuel Giner, Anthony Scemama, and Alejandro Ramírez-Solís†

CNRS-Laboratoire de Chimie et Physique Quantiques, IRSAMC, Université Paul Sabatier, 118 Route de Narbonne, 31062 Toulouse Cedex, France

**ABSTRACT:** We present a comparative study of the spatial distribution of the spin density of the ground state of $CuCl_2$ using Density Functional Theory (DFT), quantum Monte Carlo (QMC), and post-Hartree−Fock wave function theory (WFT). A number of studies have shown that an accurate description of the electronic structure of the lowest-lying states of this molecule is particularly challenging due to the interplay between the strong dynamical correlation effects in the 3*d* shell and the delocalization of the 3*d* hole over the chlorine atoms. More generally, this problem is representative of the difficulties encountered when studying open-shell metal-containing molecular systems. Here, it is shown that *qualitatively* different results for the spin density distribution are obtained from the various quantum-mechanical approaches. At the DFT level, the spin density distribution is found to be very dependent on the functional employed. At the QMC level, Fixed-Node Diffusion Monte Carlo (FN-DMC) results are strongly dependent on the nodal structure of the trial wave function. Regarding wave function methods, most approaches not including a very high amount of dynamic correlation effects lead to a much too high localization of the spin density on the copper atom, in sharp contrast with DFT. To shed some light on these conflicting results Full CI-type (FCI) calculations using the 6-31G basis set and based on a selection process of the most important determinants, the so-called CIPSI approach (Configuration Interaction with Perturbative Selection done Iteratively) are performed. Quite remarkably, it is found that for this 63-electron molecule and a full CI space including about $10^{18}$ determinants, the FCI limit can almost be reached. Putting all results together, a natural and coherent picture for the spin distribution is proposed.

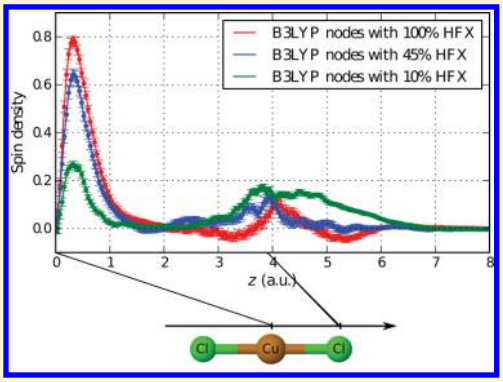


## 1. INTRODUCTION

In spite of much effort in the last 50 years, to devise a general electronic structure approach that is both computationally practical and accurate enough for all types of molecular systems is still a challenging task. Indeed, to provide a truly accurate account of the electronic structure of a molecule one must take into account in a *balanced* way several effects of different physical/chemical nature, (a) electron−electron correlation effects (resulting from the $1/r_{12}$ interaction), (b) exchange effects (Pauli principle), (c) delocalization (kinetic effects) and, in some cases, (d) quasi-degeneracy effects (quantum entanglement of almost degenerate low-energy wave function components). All the present-day methods deal with these aspects in different ways, sometimes with not so-clear distinctions between them (e.g., the mixture of exchange and nondynamical correlation effects within Kohn−Sham formulation of Density Functional theory). Here, we shall consider the two most widely used electronic structure methods, namely, Density Functional Theory (DFT) and molecular orbital-based or wave function theories (WFT) (post-Hartree−Fock approaches). We shall also consider quantum Monte Carlo (QMC) methods that are potentially very accurate but are still methods of limited use in quantum chemistry due to a number of practical/theoretical limitations. Each type of method treats the various effects cited above in different ways with particular strengths and weaknesses.

Density functional theory (DFT) is nowadays the most popular and widely used theory for the description of electronic structure of atoms, molecules, and condensed phases (solids and liquids). Its success stems mainly from the fact that it provides reasonable energetic and structural properties at a moderate computational cost. However, as well-known, many questions remain open in the DFT realm, mostly due to the necessity of approximating in a coherent way the unknown universal exact exchange-correlation functional.

In the case of WFT, the quantum chemical description passes through the construction of an explicit wave function with the need of accurately introducing static and dynamic electronic correlation effects. Ideally, this can be achieved through the construction of the Full Configuration Interaction (FCI) wave function. However, since for most molecules the FCI solution is readily out of reach even with moderate basis sets, approximate solutions are needed and are achieved in practice by building

**Received:** May 15, 2014

   dx.doi.org/10.1021/ct5004252 | *J. Chem. Theory Comput.* XXXX, XXX, XXX−XXX

increasingly complex wave functions following one of several approximations using either perturbation, truncated CI (CIS, CISD, CISDQ, CISDTQ, ...) or coupled cluster (CCSD, CCSD(T), ...) techniques. Note that, within the WFT framework, the question of whether or not the electronic state in question can be correctly described using single-reference methods also appears. In the negative case, the application of the Complete Active Space SCF (CASSCF) method has become customary and the ensuing CASSCF wave function is used as zeroth-order reference for further treatment of the dynamic correlation effects, for instance, through the CASPT2 method.

The third type of methods considered here are the so-called quantum Monte Carlo (QMC) approaches. QMC are statistical methods for solving the Schrödinger equation. They are very attractive since they are potentially exact methods (up to the statistical errors inherent to any Monte Carlo approach). Unfortunately, in practice, we have to cope with the pathological fluctuations of the wave function sign and a so-called fixed-node approximation has been introduced to fix this problem. This approximation can be viewed as solving the electronic Schrödinger equation but with a new additional constraint, namely, imposing the solution to vanish wherever a known trial wave function given as input vanishes. In other words, the nodal hypersurface of the fixed-node wave function (nodes = 3*N*-dimensional hypersurface where the wave function vanishes) are imposed to be identical to those of the approximate trial wave function. Numerical experience has shown that the fixed-node error is small according to the quantum chemistry standards (typically, a small percentage of the correlation energy for total energies) but, unfortunately, still large enough to lead to potential difficulties when computing the small energy differences involved in quantitative chemistry. Stated differently, suitable cancellation of fixed-node errors are needed. In practice, it has been observed that the nodal quality is directly related to the physical/chemical content of the trial wave function. In short, the better the trial wave function is, the smaller the fixed-node error is. Let us emphasize that the need of having a trial wave function with good nodes to start a QMC calculation brings back some heuristics into the approach, a crucial point one has to be aware of. This aspect will be exemplified here for the $CuCl_2$ molecule. Note that in the case of the transition-metal oxides a number of works investigating nodal properties of such systems have been published by Mitas et al.[1−4]

As seen, for different reasons none of these state-of-the-art approaches are fully satisfactory to deal with all types of molecular problems. Here, we propose to shed some light on their theoretical and practical relationships on a small molecule which is representative of a difficult molecular problem, namely, the ground state properties of the $CuCl_2$ molecule. As shown in previous studies, even the determination of the nature of the ground state and the proper energetic ordering of the low-lying states of this molecule turns out to be particularly difficult. This is mainly due to a subtle interplay between the delocalization of the Cu(3d) hole on the molecular axis and the dynamic correlation effects. Here, in order to investigate such relationships, we focus on the spatial distribution of the spin-density of the ground-state along the molecular axis, which is the main physical quantity associated with the relative stability of the lowest electronic states in $CuCl_2$. More precisely, we consider the difference of $\alpha$ and $\beta$ spin densities integrated within the plane perpendicular to the molecular axis (actually, a parallelepiped of small thickness). Our working definition is

$$\Delta\rho(z) = \int_{z-\epsilon/2}^{z+\epsilon/2} \mathrm{d}z \iint \mathrm{d}x\mathrm{d}y[\rho_\alpha(\mathbf{r}) - \rho_\beta(\mathbf{r})] \quad (1)$$

where $z$ is the coordinate along the molecular axis of the linear centro-symmetric molecule, the copper atom being at the origin, and $\epsilon$ is a small positive parameter (here, chosen equal to 0.1 au) corresponding to the thickness of the parallelepiped. For simplicity this partially integrated difference of $\alpha$ and $\beta$ densities will be shortly referred to in the present work as the spin density distribution. Although the DFT approaches lead to a slightly different optimized geometry (ca. 3.92−3.97 au), in what follows we shall use the equilibrium centro-symmetric geometry fixed at a Cu−Cl distance of 3.9 au, closer to the experimental value of 3.85 au for the ground state.

The contents of the paper are as follows. In Section 2, we summarize what is known about the nature of the low-lying electronic states of $CuCl_2$. Sections 3,4,5, and 6 present the results obtained for the spatial distribution of the spin density using DFT, WFT, QMC, and near-Full CI, respectively. Finally, in Section 7, a detailed summary and discussion of the results obtained is presented.

## 2. WHAT IS KNOWN ABOUT $CuCL_2$

The quantitative description of the electronic structure of metal-containing systems is known to be a rather delicate problem. The spectroscopy of $CuCl_2$ is a particularly difficult case for ab initio and DFT methods, since important correlation effects in the 3d shell of copper are strongly coupled to charge transfer effects via the 3p orbitals of the Cl ligands. Fortunately, the low-lying transitions are experimentally quite well-known[5−9] and two benchmark multireference Averaged Coupled Pair Functional studies on the spectroscopy of $CuCl_2$ exist; there the attention was focused on the nature of the three lowest electronic states[10,11] that give rise to the four observed transitions.

The first three ligand field (LF) states are thought to arise from d-d transitions on the copper ion, and they can be described by a different orientation ($\sigma$, $\pi$, or $\delta$) of the singly occupied HOMO, in principle, the localized Cu(3d) hole. So, at this point one might ask why is this such a complicated problem? In order to understand the complexity in the spectroscopic description involving the five lowest ligand-field (LF) and charge-transfer (CT) states note that, at the doubly ionic limit, $CuCl_2$ is described by the $Cl^-Cu^{2+}(3d^9)Cl^-$ structure, while in the covalent ClCuCl description, the copper atom, which is promoted to the $3d^94s^2$ excited state undergoes 4s-4p hybridization and can establish covalent bonds with both Cl atoms. An intermediate situation arises when one considers the resonant $Cl^-Cu^+(3d^94s^1)Cl$ and $ClCu^+(3d^94s^1)Cl^-$ ionic structures. Near the equilibrium geometry, the exact electronic structure for all states is a mixture of these three valence situations. The first three LF states ($^2\Sigma_g^+$, $^2\Pi_g$, $^2\Delta_g$) correspond to d-d transitions on the copper ion, and it is generally thought that they can be described by the $\sigma$, $\pi$ or $\delta$ orientations of the singly occupied Cu(3d) orbital. It is known that a correct description of electronic structures, and even more with such close lying states, must include a correct description of correlation effects especially important for the d shell, but also must allow for large repolarization differential effects between localized d-d states and charge transfer states. We


dx.doi.org/10.1021/ct5004252 | J. Chem. Theory Comput. XXXX, XXX, XXX−XXX

stress that single-reference methods such as Coupled Pair Functional(CPF) and CCSD(T) can be used here, since the HF wave functions are excellent zeroth-order approximations for the lowest electronic states of $CuCl_2$.[12] From the DFT perspective, this feature is also very convenient, since standard Kohn–Sham based methods are well adapted to describe transitions where only a change in the orientation of the 3d-hole in the central metal atom is involved. We stress that the $^2\Pi_g \rightarrow {}^2\Sigma_g^+$ transition in $CuCl_2$ represents a most difficult problem from the quantum theoretical point of view, since it has been predicted to range from −2495 to 6930 $cm^{-1}$.[13]

Table 1 presents some selected DFT (LDA, GGA, hybrid. and meta) and the ab initio $^2\Pi_g \rightarrow {}^2\Sigma_g^+$ transition energies

**Table 1. DFT, Ab Initio, and Experimental Transition Energies in Wavenumbers, Mulliken Spin Densities (SD) on the Cu Atom Where Available**

| method | $^2\Pi_g \rightarrow {}^2\Sigma_g^+$ | $^2\Pi_g$ SD | $^2\Sigma_g^+$ SD |
|---|---|---|---|
| LDA(S+VWN5) | 6539 | 0.316 | |
| BLYP | 4802 | 0.429 | 1.04 |
| PBE96 | 4699 | 0.43 | 1.03 |
| HCTH407 | 4345 | 0.420 | |
| OPTX-LYP | 3963 | | |
| TPSS | 4065 | 0.406 | |
| M06-2X | 3251 | 0.648 | |
| B3LYP | 1703 | 0.57 | 1.07 |
| B97-2 | 1465 | 0.54 | 1.03 |
| PBE0 | 756 | 0.64 | 1.08 |
| NR-SCF[a] | −2495 | 0.962 | |
| CASSCF(21,14) | 6930 | 0.94 | 1.00 |
| CASSCF+ACPF | 232 | | |
| CASPT2 | 3861 | | |
| NR-SDCI[a] | −2116 | | |
| NR-SDCI+Q[a] | −1856 | | |
| CCSD(T) | 859 | | |
| NR-Coupled Pair Functional[a] | 659 | | |
| theor.[b] | 900 | | |
| expt.[c] | 253, 303, 475 | | |

[a]Nonrelativistic all-electron calculations from ref 12. [b]Theoretical spin–orbit deconvoluted value from ref 10. [c]Experimental fine-structure transition energies; see corresponding references in ref 13.

along with the corresponding spin densities on the central Cu atom. Basis sets used for such calculations are those reported in the previous work,[13] namely, extended valence basis sets of (9s11p8d6f4g)/[8s9p6d2f1g] quality for Cu and of (6s6p5d4f)/[5s5p2d1f] type for Cl coupled to the Stuttgart-Köln RECP. Previous results from nonrelativistic calculations are also reported using large ANO-type basis sets for both atoms.

Note that, within the ab initio framework, the dynamic correlation effects that control the nature of the Cu 3d-hole in the ground state are extremely difficult to obtain correctly since the SCF, the SDCI, and even the usually very accurate SDCI +Q (with Davidson's approximate size-consistent correction) schemes, all wrongly lead to a $^2\Sigma_g^+$ ground state. Only more sophisticated size-consistent ab initio methods such as CPF, CCSD(T), or CASSCF+ACPF are able to correctly predict a $^2\Pi_g$ ground state, lying 659, 859, and 232 $cm^{-1}$ (respectively) below the $^2\Sigma_g^+$ one without spin–orbit (SO) effects. Note that, at the purely electronic level, transition energies must be compared with the theoretical SO-deperturbed value, estimated to be 900 $cm^{-1}$.[10] We also stress that Bauschlicher and Roos[12] showed that the Darwin and mass-velocity relativistic effects cancel out nicely for the spectroscopy of this molecule and were thus able to use all-electron nonrelativistic (NR) calculations. From the DFT perspective, most functionals (GGA, hybrid and even meta-ones) such as HCTH407, BLYP, PBE96, OptX-LYP, TPSS, and M06-2X largely overestimate this transition, all yielding values above 3200 $cm^{-1}$. Note that up to date, it is impossible to decide a priori which functional is to be used and which one can be trusted to yield reliable transition energies for an arbitrary metallic molecule. The delicate issue of the parametrization of most exchange-correlation functionals without the inclusion of transition metal containing systems has been discussed[13] in this context. It is somewhat ironic that much less expensive and sophisticated descriptions such as those given by the PBE0 (750 $cm^{-1}$) and the B97-2 (1400 $cm^{-1}$) functionals yield better approximations to this transition energy than the very computational demanding benchmark CASSCF+ACPF one at 232 $cm^{-1}$. So, the natural question arises: Are these hybrid PBE0 and B97-2 densities correctly describing each electronic state, therefore providing truly accurate total energies, or is this energy difference hiding some cancellation of errors associated with physically relevant quantities, such as the spatial distribution of charge and spin densities?

Although the various results presented in Table 1 may appear rather diverse, one might observe a correlation of the amount of HFX with the energy difference between the lowest states, although this is not strictly satisfied in all cases due to the coupling of the exchange and correlation functionals in each case. In the extreme case of SCF-HF, we find the largest (negative) transition energy with $^2\Sigma_g^+$ state as the ground-state. In the opposite case where no HF exchange is included (BLYP, for instance), the $^2\Pi_g^+$ state becomes the ground state with a large (positive) transition energy. In between, one can see that for functionals having a fraction of HF exchange, this transition energy is still positive but smaller. To illustrate quantitatively this idea we present in Figure 1, for the B3LYP functional with variable HF exchange, the evolution of the transition energy vs the HF exchange percentage.

This figure illustrates in a particularly striking way the high level of arbitrariness present when using hybrid functionals, such as B3LYP, for this system. Clearly, there is no rational way to decide which is the "right" amount of HF nonlocal exchange to be used.

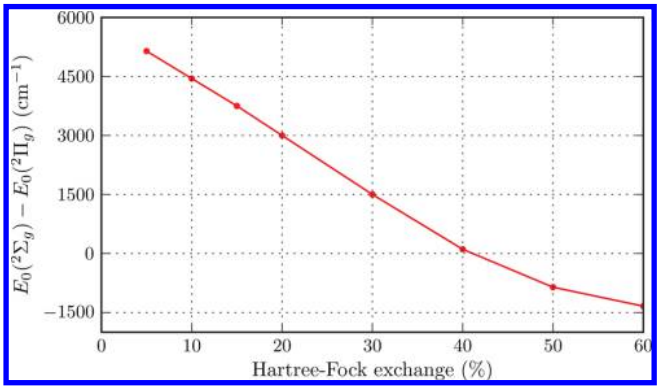


**Figure 1.** $^2\Pi_g \rightarrow {}^2\Sigma_g^+$ transition energy (wavenumbers) with B3LYP as a function of the HF exchange percentage employed; positive values correspond to a $^2\Pi_g$ ground state, in agreement with experiment.


dx.doi.org/10.1021/ct5004252 | J. Chem. Theory Comput. XXXX, XXX, XXX–XXX

Another quantity related to this aspect (via the localization of the 3d hole) is the spin-density on the central copper atom. In Table 1, we present the values of several LDA, GGA, and hybrid DFT-derived Mulliken spin-densities (SD) on the central Cu atom and the ab initio CASSCF values for both states, each at its equilibrium geometry. Note that both CASSCF wave functions were optimized considering 21 active electrons (11 from Cu and 5 from each Cl atom) in 14 active orbitals (3p of Cl and 3d,4s,4p of Cu, and one active orbital removed; see ref 14) leading to large expansions with about 23 000 CSF. Clearly, a rather different picture of the spin-density distribution is obtained with the DFT-derived methods vs the corresponding ab initio ones, especially for the $^2\Pi_g$ ground-state. It is quite remarkable that the quality of the excitation spectrum obtained with these functionals can be related to the magnitude of the spin-density on the central metal atom, since although all the functionals yield SD(Cu) values close to 1.0 for the $^2\Sigma_g^+$ state, the corresponding value for the $^2\Pi_g$ ground state shows large variations between the good and bad-performing functionals. The PBE0 SD(Cu) value is 0.64, while the BLYP and PBE96 spin-densities on copper are only 0.43. An intermediate situation arises for the next two best performing functionals, B3LYP and B97-2, with larger values of 0.57 and 0.54. The CASSCF(21,14) spin-densities are both very close to 1 for both electronic states, and this is precisely why it is generally thought that these ligand states actually present a much more localized hole on the central copper atom than any of the DFT descriptions provide. We shall address this important point in more detail in what follows.

## 3. GROUND-STATE SPIN DENSITY WITH DFT

Having in mind the previous results, we start our analysis of the ground state spin density along the molecular axis with the DFT approaches. Note that the singly occupied molecular orbital (SOMO) plays a central role for many of the chemical/physical properties of the molecule. It is so since in the spin-restricted Kohn−Sham formalism the contribution to the spin density resulting from all lower-lying orbitals cancels out and the local spin density is directly written as the square of the singly occupied orbital (other orbitals also contribute but in an indirect way through the Kohn−Sham optimization). The $\sigma$ or $\pi$ symmetry of the SOMO defines the overall symmetry of the ground state. In Figure 2, the SOMO orbitals obtained with B3LYP for the $^2\Pi_g$ ground state as a function of the internuclear axis $z$ for different values of HF exchange percentage are shown, along with the ROHF orbital. The atomic basis sets used here and in the following section are extended all electron basis sets of (21s,15p,10d,6f,4g)/[8s,7p,5d,3f,2g] quality for Cu[15] and of (17s,12p,5d,4f)/[6s,5p,3d,2f] quality for Cl from ref 16. Since these orbitals are centro-antisymmetric with respect to the Cu atom, only the $z > 0$-region is shown. In this figure, the $y$ coordinate is fixed to zero and $x$ to 0.15, a value close to the maximum of the highest peak of the orbital. Figure 3 gives the B3LYP spin-densities obtained as a function of the HF exchange percentage together with the HF spin density.

The two-peak structure of the SOMO (Figure 2) and $\Delta\rho(z)$ in Figure 3 is clearly seen, one peak localized very close to the central Cu atom and the other on the chlorine atom. The relative height between the two maxima is strongly dependent on the percentage of HF exchange considered. In the case of HF, the main peak is the highest one while the secondary peak on Cl is 20 times smaller. This indicates a highly localized

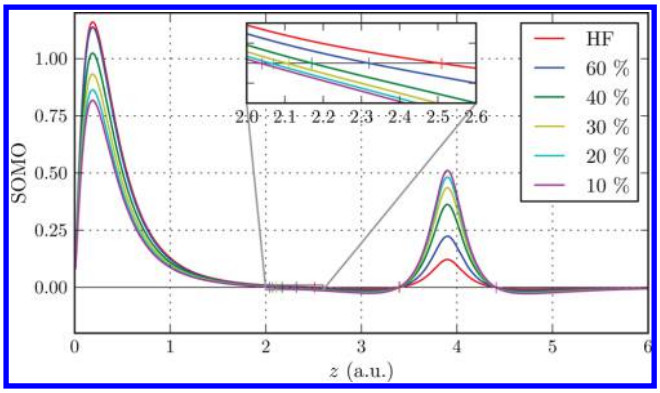


**Figure 2.** Plot of the singly occupied molecular orbital along the nuclear axis $z > 0$ (copper at origin and chlorine at $z = 3.9$ au) for the $^2\Pi_g$ ground-state using B3LYP as a function of the HF exchange percentage used in the hybrid functional. The values of $x$ and $y$ are fixed to 0. and 0.15, respectively. The inset is a blow-up of the region in the middle of the bond where the SOMO vanishes. See discussion in Section 5.

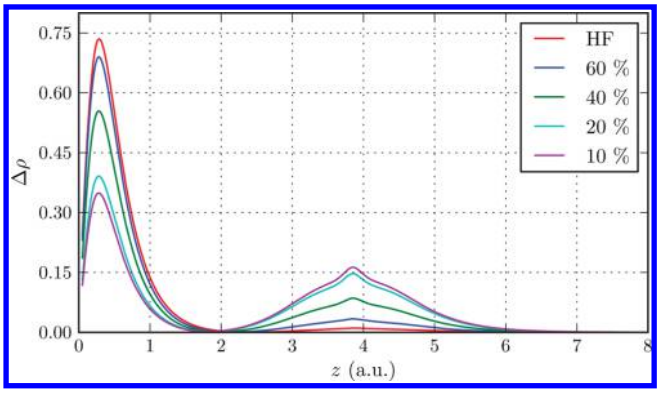


**Figure 3.** Ground-state spin density with B3LYP as a function of the HF exchange percentage. Cu at the origin and Cl atoms located at $z = \pm 3.9$ au; only the positive $z$ axis is shown.

character for the 3d hole at the HF level. When decreasing the percentage of HF exchange in B3LYP, the level of localization is found to decrease uniformly. Note also that the location of the zero (node) of the SOMO in the middle of the bond (blow-up in Figure 2) is very dependent on the amount of HF exchange. This result will be discussed in the context of the FN-DMC results (see Section 5). As in the case of the $^2\Sigma_g$-$^2\Pi_g$ transition energy presented above, there is no physically meaningful reason to decide which amount of nonlocal HF exchange should be used in B3LYP for this metallic system.

## 4. GROUND-STATE SPIN DENSITY WITH WFT: HF AND BEYOND

Let us now turn our attention to the spin densities obtained from wave function approaches (WFT) at different levels of theory. Figure 4 shows $\Delta\rho(z)$ obtained for the $^2\Pi_g$ ground-state using both ROHF and CASSCF calculations. In the later case, the active space chosen includes 14 orbitals (3p shell of both Cl, 4s, 4p, and 3d shells for Cu, one active orbital removed[14]) and 21 valence electrons (5 from each Cl and 11 from Cu) are distributed among them. In the resulting CASSCF(21,14) expansion the HF coefficient is found to be rather large (0.95), thus indicating a strong single-reference character of the ground-state wave function. Therefore, dynamic correlation


dx.doi.org/10.1021/ct5004252 | J. Chem. Theory Comput. XXXX, XXX, XXX−XXX

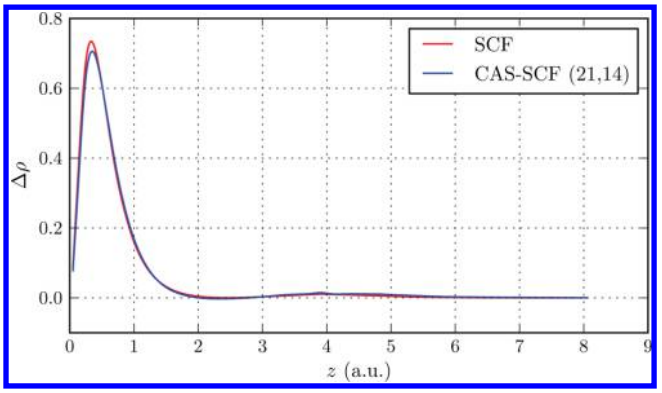


**Figure 4.** $^2\Pi_g$ state spin density along the molecular axis (in au) at the HF-SCF and CASSCF levels.

effects largely dominate this problem. Note that the CASSCF spin-density distribution presented has been obtained by considering only the first one hundred determinants corresponding to the largest coefficients in the expansion. As seen in Figure 4 and expected from the single-reference nature of the wave function, HF and CASSCF spin-densities are almost identical. In both cases, the 3d hole is found to be strongly localized on the copper atom and almost no spin density is present on the chlorine atoms.

As shown in Table 1, only the use of highly correlated methods (CCSD(T), CPF, or ACPF) can recover the correct energetic ordering of the two lowest electronic states. Unfortunately, given the huge number of CSF (ca. $7 \times 10^9$) considered in these approaches, the spin density distributions at these levels of theory are not available.

## 5. GROUND-STATE SPIN DENSITY WITH QUANTUM MONTE CARLO

In this section, we report all-electron quantum Monte Carlo (QMC) calculations of spin-densities. Several versions of QMC have been introduced in the literature; however, they all rely on the same ideas and differ only by technicalities. Here, we employ a variant of the Fixed-Node Diffusion Monte Carlo (FN-DMC) method defined with a constant number of walkers. For details, the interested reader is referred to the original work.[17] In FN-DMC we are faced with two main sources of error: the statistical error inherent to any Monte Carlo approach and the fixed-node error. Other sources of errors are also present, but they can be easily controlled and made negligible (see, ref 18). By increasing the number $N$ of Monte Carlo steps the $1/\sqrt{N}$-statistical error can be decreased as much as desired, at least in principle. In each application presented below, this error has been reduced to a level sufficient for our purposes. In contrast, the fixed-node approximation is much more challenging and its control is a crucial issue of present-day QMC approaches. It is known that the magnitude of the fixed-node error is directly related to the quality of the nodal structure of the approximate trial wave function used in the simulation [the nodes are the $(3N - 1)$-dimensional zeroes of the $3N$-dimensional wave function, $N$ being the number of electrons]. Exact total energies can be obtained only when using trial wave functions having the nodes of the exact (unknown) wave function. It should be emphasized that, in contrast with the statistical error which can be reduced as desired by increasing Monte Carlo statistics, the fixed-node error is a *systematic error* (i.e., a bias) that survives even for infinite statistics. Numerical experience has shown that, although fixed-node energies are very accurate, non-negligible errors on energy differences may still occur due to improper cancellation of fixed-node errors. Unfortunately, in some cases this error can be large enough to lead to *qualitative* wrong conclusions. When considering closed-shell systems with a strong single-reference nature, nodal hypersurfaces resulting from single-determinant representations (e.g., Hartree−Fock or Kohn−Sham type) are expected to be of sufficient quality. As we shall see, in the $CuCl_2$ case considered here, the situation is different. Although the exact wave function has a strong single-reference character, the presence of an open-shell makes the nodal structure of the wave function more difficult to describe. In this case, the nodes of the $3N$-dimensional wave function turn out to be very sensitive to the 3-dimensional nodal pattern chosen for the singly occupied molecular orbital (SOMO). Note that it is an interesting case where the highly complicated $3N$-dimensional nodes usually so difficult to visualize can be reduced, in a good first approximation, to a much simpler 3D-pattern.

A last point to specify is the way spin-densities are computed here. In the case of total energies, it is known that the only systematic error is the fixed-node one, despite the fact that the stationary diffusion Monte Carlo distribution is not exact. DMC actually samples the so-called mixed distribution given by the product of the trial wave function and the exact wave function; see ref 18. In the case of properties other than energies, this is no longer true and some additional error related to the trial wave function contribution in the mixed distribution is present. This error can be removed in different (costly) ways; see for example refs 19 and 20. However, such a possibility was not considered here since, as we shall see later, the dominant source of error is the fixed-node approximation. Spin-densities are thus calculated in a standard way using a hybrid second-order estimate. Precisely, the average value of a general observable $O$ is evaluated as[21]

$$\langle O \rangle \sim 2\langle O \rangle_{\mathrm{DMC}} - \langle O \rangle_{\mathrm{VMC}} \tag{2}$$

where averages are taken either over the mixed distribution sampled in DMC or over the squared trial wave function density sampled in a variational Monte Carlo (VMC) simulation. Here, the properties to be computed are the $\alpha$ and $\beta$ spin densities and the quantities to average are merely the number of $\alpha$ or $\beta$ electrons falling within histogram bins.

The all-electron Fixed-Node DMC spin-density for the $^2\Pi_g$ ground-state using a Hartree−Fock wave function as trial wave function (complemented with a standard Jastrow factor to reduce statistical fluctuations for the energy) is presented in Figure 5. The basis set used is that presented in previous section 3. For comparison, the Hartree−Fock spin density is also given. Although some differences between the two curves exist, they should essentially be considered as the same when compared to the typical differences present in the DFT-spin density curves; see Figure 2. The small differences include a slight increase of the main DMC peak and a small "spin-density wave" around Cl atoms. In this calculation, the total energies obtained at the SCF and FN-DMC levels are −2558.1050 au and −2560.719(2) au, respectively. To get an assessment of the accuracy reached here with QMC a rough estimate of the exact total energy of the molecule can be done. For that, we add to the sum of atomic energies the atomization energy calculated at the SCF level. Taking for Cl the value from Davidson et al.,[22] for Cu the HF energy of Bunge,[23] plus the correlation energy


dx.doi.org/10.1021/ct5004252 | J. Chem. Theory Comput. XXXX, XXX, XXX−XXX

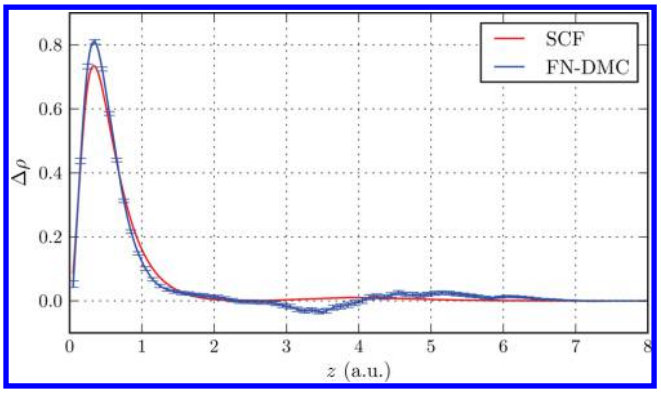


**Figure 5.** $^2\Pi_g$ state spin density along the molecular axis (in au) at the FN-DMC level with a HF trial wave function.

estimate of Clementi et al.,[24] the exact energy of separate atoms is found to be about −2560.868 au. Adding the SCF atomization energy, we get a total ground-state energy for $CuCl_2$ of about −2561.045 au. The percentage of correlation energy recovered by FN-DMC with HF nodes is thus quite large, roughly ∼89%. Thus, with this highly correlated description of the wave function but imposing HF nodes, it is found that the shape of the spin density distribution is not quantitatively changed with respect to that obtained at the SCF level.

Let us now consider the FN-DMC spin-densities obtained when using KS determinants instead of the Hartree−Fock one as trial wave functions. The KS determinants were obtained with standard B3LYP and with B3LYP with a variable amount of HF exchange. In Figure 6, the corresponding FN-DMC spin-densities are presented.

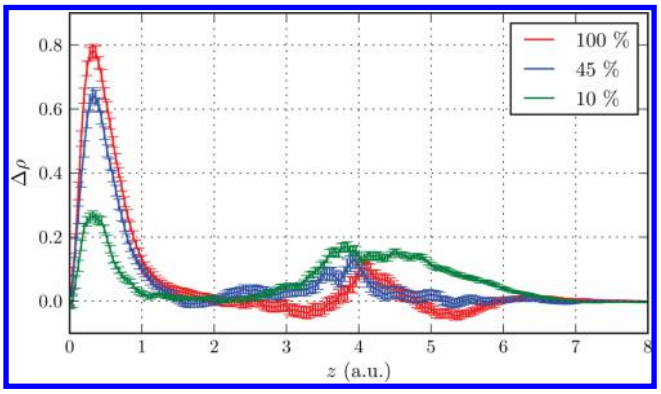


**Figure 6.** $^2\Pi_g$ state FN-DMC spin densities along the molecular axis (in au) using as trial wave function B3LYP-KS determinants obtained with different amounts of HF exchange.

As clearly seen, the overall shapes of FN-DMC spin-densities are tightly correlated with those obtained at the corresponding DFT level; see Figure 3. The results are thus similar to what has just been obtained for the SCF case: No qualitative change of the spin densities is obtained when passing from the variational to the FN-DMC level. These results strongly suggest that the key factor determining the spin density profile is the nodal structure of the trial wave function used. The situation can thus be summarized as follows: (i) the amount of Hartree−Fock exchange in B3LYP determines the relative weight of $3p_{Cl}$ and $3d_{Cu}$ atomic contributions to the SOMO (ii) the nodes of the SOMO are directly related to this relative weight, and (iii) the nodal pattern of the whole trial wave function is dominated by the SOMO nodes. In the inset of Figure 2, a blow-up of the SOMO in the region around its node located at the middle of the Cu−Cl bound is presented; the two other nodes close to the secondary peak are weakly dependent on the level of exchange and will not be discussed here. The position of the central node is seen to be very sensitive to the percentage of HF exchange. Its location ranges from $R_{node}$ = 2.5 a.u. for the Hartree−Fock wave function to about 2.05 a.u. for the KS determinant corresponding to the lowest HF percentage of 10%. In short, the nodes of the trial wave function are very sensitive and directly related the amount of HF exchange chosen. At this point, the situation is clearly not satisfactory, since the overall shape of spin distributions is determined by the specific choice of nodes of the SOMO. Said differently, FN-DMC is not able to change qualitatively the global features of the spin-density associated with the approximate trial wave function given in input for the diffusion Monte Carlo process. We thus need to resort to alternative approaches capable of changing the nodes when electronic correlation effects are included. This will be the subject of the following section. Before that, let us nevertheless note that there exists in FN-DMC an internal criterion for estimating the nodal quality. It is based on the variational principle stating that the "better" the nodes are, the lower the fixed-node energies are expected to be.[21] Figure 7 presents the variation of the total FN-DMC

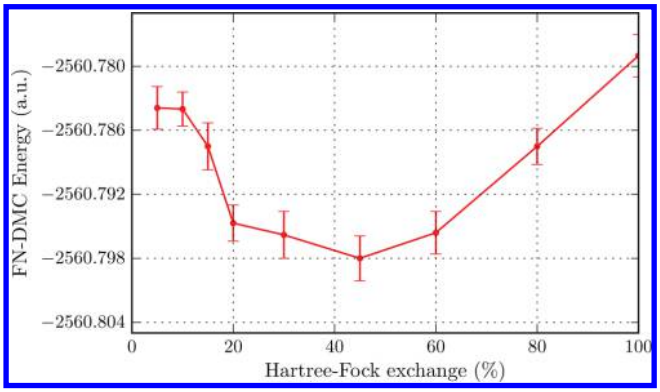


**Figure 7.** Total FN-DMC $^2\Pi_g$ ground state energy obtained with a B3LYP determinant as a function of the HF exchange percentage for $CuCl_2$.

ground-state energy as a function of the amount of exchange considered. Note that the use of such a criterium has already been employed by Kolorenč and coll.[4] The basis set employed in these calculations is that of Weigend and Ahlrichs,[25] which leads to significantly lower fixed-node energies than those obtained with the basis set used in refs 10 and 11. Quite remarkably, a minimum is observed for a HF exchange percentage around 45%. This result is interesting and may be understood as a first indication of the typical amount of HF exchange that should be employed. However, let us stress that this result must be considered with lot of caution since the sensitivity of the FN-DMC results on nodal choice is high and optimizing only the one-dimensional nodes of the SOMO could be insufficient. Furthermore, optimizing nodes via minimization of the total energy is not a guarantee of improvement for other properties such as spin density distributions.


dx.doi.org/10.1021/ct5004252 | J. Chem. Theory Comput. XXXX, XXX, XXX−XXX

## 6. GROUND-STATE SPIN DENSITY WITH NEAR-FCI

In this section, we report near-Full Configuration Interaction (FCI) calculations for total energies and spin-densities. To achieve converged results on this system including 63 electrons, a small 6-31G basis set is employed for both atoms, leading to a molecular basis of 55 orbitals. Clearly, the quantitative accuracy reached with such a modest basis set can be questioned. However, it will allow us to calculate the spin densities, the energy gap, and their evolution upon the number of determinants considered, in a case where the wave function includes most electronic correlation effects (although semi-quantitatively), either static or dynamical. As we shall see, despite their semiquantitative nature, FCI/6-31G results will indeed provide us with important information about the origin of the conflicting results obtained with the previous approaches.

To realize FCI-type calculations for this system, we use the CIPSI approach (Configuration Interaction with Perturbative Selection done Iteratively), a method proposed more than four decades ago (see, refs 26 and 27, and references in 28) and very recently introduced in the context of QMC approaches.[28] For a detailed presentation of this approach, the reader is referred to the original works. In short, CIPSI is a variational and multireference perturbational configuration interaction approach in which determinants that are to be included in the variational space are selected iteratively according to an energy criterion. Determinants perturbationally generated are added to the variational wave function when their perturbative contribution to the total energy is greater than a given threshold. In contrast with standard CI approaches where a whole set of particle-hole excitations are considered (single-excitations, single- and double-excitations, etc.), only excitations having a significant impact on the wave function expansion are selected as variational contributions. The relevance of a particular excitation is decided by comparing its energy contribution with the prefixed threshold. This procedure is applied iteratively until a given target number of determinants is reached. In practice, this leads to rather compact variational expansions consisting of a limited number of determinants in each type of excitations. Furthermore, higher-degree excitations not usually present in standard CI expansions may also be naturally introduced in the variational space with the CIPSI approach. Finally, let us note that several applications for a variety of metal-containing molecules have been realized during the 90s; see for example refs 29−35. The major difference between these applications and the present study is the size of the variational space that is taken much larger here (up to a million of determinants). The second-order perturbational correction is thus much reduced and an accuracy close to the FCI limit can be reached in the present application.

In Figure 8, the convergence of the ground-state energy as a function of the number of determinants kept in the variational space is presented. To reduce the size of the CI calculation, molecular orbitals of the neon and argon cores for the chlorine and copper atoms, respectively, have been kept frozen (a total of 19 orbitals and 38 core electrons). Calculations have been performed using as active molecular orbitals the 36 remaining orbitals (all valence and virtual molecular orbitals) and the remaining 25 valence electrons. We stress that the size of the full CI space is about $10^{18}$ determinants. With the present basis set the maximum number of determinants in the variational space considered here is $10^6$. The three upper curves of Figure 8 are the variational energy curves corresponding to the

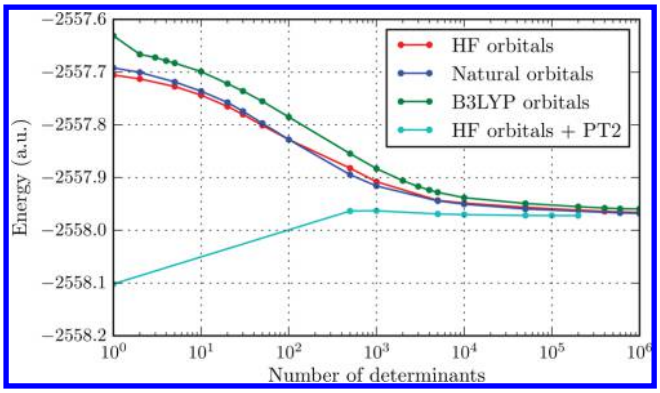


**Figure 8.** Total variational (three upper curves) and variational + perturbational (lower curve) ground-state energy as a function of the number of determinants kept in the CIPSI selection process. SCF, B3LYP, and natural orbitals are used.

multideterminantal expansion, $|\Psi_0\rangle$ built using either SCF, DFT-B3LYP, or natural molecular orbitals. The latter were constructed from the variational CIPSI wave function obtained with $10^6$ determinants. As seen on the figure, all curves are found to converge almost to the same value, as it should be when approaching the full CI limit. The lower curve shows the so-called CIPSI energy obtained by adding to the variational energy $E_0$ the second-order perturbative contribution defined as

$$E_{PT2} = -\sum_{i\in P} \frac{\langle \Psi_0|H|D_i\rangle^2}{\langle D_i|H|D_i\rangle - E_0} \quad (3)$$

where $P$ denotes the set of all determinants not present in the multideterminantal expansion $|\Psi_0\rangle$ but connected to it by the Hamiltonian $H$ (single- and double-excitations). For clarity only the CIPSI curve obtained with HF orbitals is shown, the other CIPSI curves having a similar behavior. $E_{PT2}$ can be considered as a measure of the energy difference between the variational energy and FCI limit. As seen on the figure, the convergence of CIPSI energy is particularly rapid, we consider the limit has been attained with about 50 000 determinants in the variational space. For a large enough number of determinants, the perturbative correction $E_{PT2}$ becomes quite small, this being a reliable indicator of the convergence to the FCI limit.

In Figure 9 the energy difference between the $^2\Sigma_g$ and $^2\Pi_g$ states as a function of the number of determinants is presented

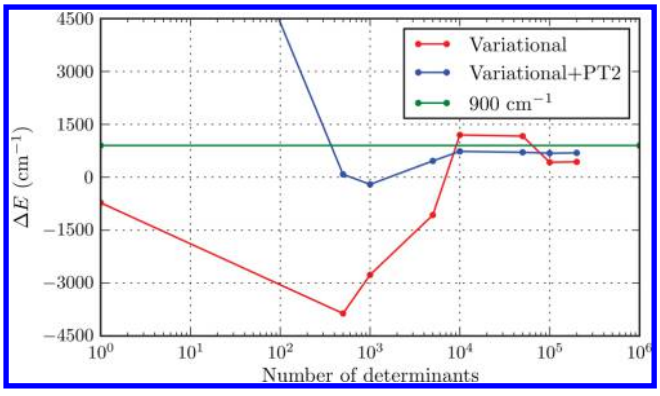


**Figure 9.** $^2\Sigma_g$–$^2\Pi_g$ energy gap as a function of the number of determinants in the variational space. The horizontal line at 900 cm$^{-1}$ is the correct spin−orbit deperturbed gap value as estimated in ref 10.


dx.doi.org/10.1021/ct5004252 | J. Chem. Theory Comput. XXXX, XXX, XXX−XXX

(note the logarithmic scale for the number of determinants). The evolution of the energy difference is shown both for the variational energies and the CIPSI energies (variational + $E_{PT2}$). At the purely variational level the $^2\Sigma_g$–$^2\Pi_g$ gap starts with a negative value (as it should be for one-determinant SCF wave functions; see Table 1) and then changes sign when about 6000 determinants are included. At small number of determinants the change in variational energy difference is important (transient regime) but at larger numbers (say, beyond $10^4$ determinants) an onset of convergence is observed. For $10^5$ and $2 \times 10^5$ determinants the variational value for the energy difference is close to 430 $cm^{-1}$. At the CIPSI level, the curve is much better behaved and the convergence is clearly reached beyond $10^4$ determinants; a value of about 690 $cm^{-1}$ is obtained. The fact that both variational and CIPSI limits are close to each other (the difference of 260 $cm^{-1}$ is small with respect to the large variations observed in energy differences calculated from various theoretical approaches) is a good indication that the variational curve has also entered a quasi-convergence regime. Note that for a small number of determinants the second-order energy correction is large and unphysical. CIPSI results are only meaningful in the large number of determinants regime, where the second-order contribution is indeed a correction.

Results obtained for the energy are very satisfactory; they demonstrate that nearly-FCI calculations are able to describe the transition between the two lowest electronic states despite the smallness of the basis set, since the converged value obtained for the energy difference is close to the estimated SO-deperturbed value of about 900 $cm^{-1}$.

For a deeper analysis, we have also calculated the spin-density obtained from the CIPSI variational wave function. Its evolution as a function of the number of selected determinants is plotted in Figure 10. As usual, a two-peak structure is

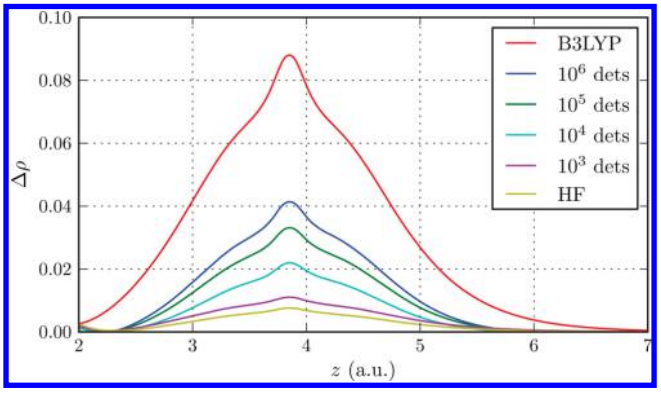


**Figure 10.** $^2\Pi_g$ state. Spin density around the chlorine atom with HF, B3LYP, and CIPSI with varying number of determinants. The basis set employed is 6-31G.

observed. In the figure, only data for the secondary peak on the chlorine atoms are shown. For comparison, the spin density distribution obtained at the SCF (nearly vanishing small peak) and B3LYP levels (the highest peak) are also plotted. Remark that the maximum of the B3LYP peak is about 0.087, to be compared with the value of 0.15 for the very same quantity presented in Figure 3 (ordinary B3LYP with 20% of HF exchange). This difference is due to the smallness of the 6-31G basis set. Using much larger basis sets, as the one used for Figure 3, we have verified that the maximum value indeed converges to 0.15. The CIPSI spin densities lie between both extreme curves and the height of the spin density peak is found to increase continuously with the number of determinants in the variational space. For the largest number of determinants in the variational space ($10^6$), the height of the peak is not yet fully converged but is large and represents about 40% of the B3LYP peak.

In Figure 11, we present a more complete view of the convergence of the secondary peak as a function of the number

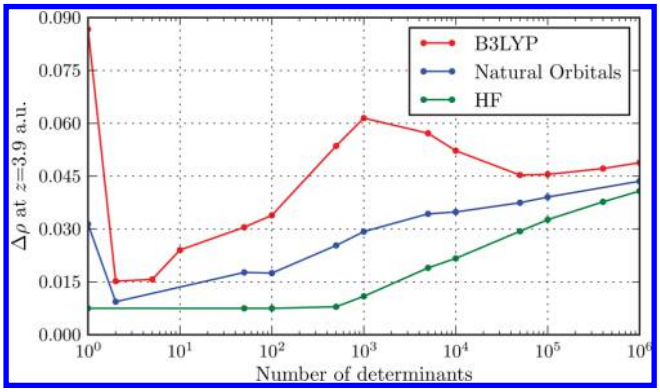


**Figure 11.** $^2\Pi_g$ state. Convergence of the maximum of the secondary peak of the spin distribution as a function of the number of determinants in the variational space. Different types of molecular orbitals were used.

of determinants selected and with various types of molecular orbitals used in CIPSI. When using HF molecular orbitals, the spin density at $z$ = 3.9 au, $\Delta\rho(3.9)$, is found to remain close to zero up to a thousand of determinants, and then, it begins to increase uniformly until it attains its maximum value. With B3LYP molecular orbitals, the situation is qualitatively different. Starting from one determinant from a high value of the peak (as shown above with the B3LYP KS determinant), it decreases rapidly to a value close to zero. This phenomenon can easily be explained by noting that in a CI calculation the role of the first determinants consists essentially in lowering the energy via single-excitations whose effect is to optimize in an effective way the (natural) one-body orbitals (here, going from pure KS to SCF-type orbitals). Because of that, $\Delta\rho(z = 3.9)$ is first found to almost vanish as in a SCF calculation. Next, when more determinants are added to the variational wave function, dynamical correlation contributions begin to appear (typically, through two-particle excitations) and then $\Delta\rho(z = 3.9)$ starts to increase. Directly using natural orbitals, a similar phenomenon occurs but in a less pronounced way, since the initial value is smaller than in the DFT case.

To support the previous scenario regarding the role of single-excitations, we present in Figure 12 the shape of the secondary peak for a small number of determinants (about 50 determinants) using natural orbitals and including or excluding the SOMO-LUMO single-excitation that enters first in the variational space. Using only one determinant built with natural orbitals the maximum found for the peak is about 0.035, the largest value of the figure. Now, a small CIPSI calculation including only 50 determinants in the variational space is performed. Two situations are considered depending on the fact that the determinant representing the SOMO-LUMO single-excitation is removed or not from the variational expansion. In the first case, the peak is essentially unchanged. In sharp contrast, in the second case the peak of the spin distribution is significantly reduced and many additional


dx.doi.org/10.1021/ct5004252 | J. Chem. Theory Comput. XXXX, XXX, XXX–XXX

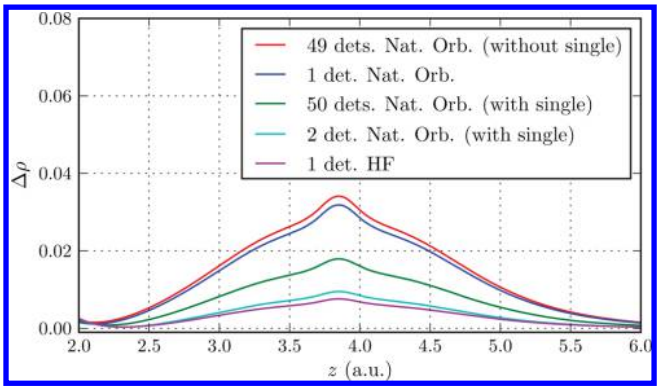


**Figure 12.** Comparison of the secondary peak of the spin density $\Delta\rho(z = 3.9)$ obtained with a small number of determinants, including or excluding the SOMO-LUMO single-excitation.

determinants are needed to recover its original shape. These results nicely illustrate the role of single-excitations recovering the Hartree−Fock nature of the orbitals when a small number of determinants is considered in the reference space.

## 7. SUMMARY

In this work, calculations of the total energy and spin-density for the $^2\Pi_g$ ground state of the $CuCl_2$ molecule have been presented using various quantum-mechanical methods. Depending on the approach employed different qualitative and quantitative descriptions of the spatial distribution of the spin density along the molecular axis have been found. At the root of such discrepancies lie the different ways the electronic structure is described and approximated.

At the DFT level, the description of the low-lying states of the molecule is very dependent on the type of exchange-correlation functional chosen. Recalling that hybrid functionals had been shown to provide the best agreement with experimental data, the transition energy between the two lowest states, $^2\Pi_g$ and $^2\sum_g$, is found to be very sensitive on the fraction of HF exchange used in the functional. For B3LYP, the gap is roughly linearly dependent on this fraction, starting from a $^2\sum_g$ ground-state with 100% HF exchange to a $^2\Pi_g$ ground state with a sufficiently low percentage (about 40% and less). Regarding the spatial distribution of the spin density, a strong dependence on the fraction of HF exchange used in the hybrid functional is found. In the case of the $CuCl_2$ molecule having a single unpaired electron, the DFT spin density is entirely determined by the square of the SOMO orbital. By varying the HF exchange percentage, the shape of this orbital may be continuously varied and so is the spin density. With the full HF exchange, the DFT spin-density is almost entirely localized on copper, while lower levels of HF exchange lead to increasingly delocalized spin densities on both Cl ligands. Such results are clearly disturbing, since there exists no internal criterion within hybrid DFT schemes to decide which amount of HF exchange should be used, and thus, a meaningful chemical picture of the electronic distribution is difficult to obtain. We recall that in the DFT framework the self-interaction error (SIE) is known to be directly related to the exchange part of the functional; in the case of the metal-containing molecules with a high electronic density in the *d* shell, this error may be particularly important and not easy to control, thus leading to a potentially incorrect description of the delocalization of electronic distributions.

A common way of shedding light on a situation where DFT leads to unpredictable results is to resort to highly correlated post-Hartree−Fock methods where the construction of accurate 3*N*-dimensional wave functions allows, in principle, a better control of the details of the electronic structure. At the HF level, and in agreement with hybrid DFT results with full HF exchange, the spin density is found to be completely localized on the central copper atom. At the CASSCF level including all Cl(3p) and Cu(3d,4s,4p) orbitals as active orbitals, the wave function is not significantly changed and is largely dominated by the HF determinant. In other words, the dynamical correlation effects dominate here and the spin density calculated with CASSCF is practically identical to that of the HF description. Unfortunately, as illustrated by a number of works, it is very difficult to reproduce with sufficient accuracy the dynamical correlation effects and thus to give a quantitative description of the low-lying states; in particular, to obtain the correct energy difference between the two lower states requires very high level calculations [e.g., CCSD(T) or ACPF] with large optimized basis sets. Unfortunately, these methods do not provide the final electronic density that would allow us to conclude on the true chemical picture concerning the spin density.

To escape from such limitations, we have utilized QMC calculations that are known to be particularly accurate. Using different types of trial wave functions fixed-node DMC calculations of both ground-state total energies and spatial distributions of the spin density have been thus obtained. Unfortunately, although we get state-of-the-art total energies (with around 90% of the total correlation energy), spin densities calculated within the fixed-node approximation are found to be too dependent on the nodal structure of the trial wave function employed. In the present case with a singly occupied molecular orbital, the complex 3*N*-dimensional nodal hypersurface of the full trial wave function is dominated by the 3-dimensional nodes of the SOMO and that the shape of the FN-DMC spin densities calculated is directly related to the shape of this orbital. Thus, qualitatively different spin density distributions can be obtained even at the supposedly very accurate FN-DMC level, depending on the choice of the singly occupied orbital used in the trial wave function. Using a HF-type wave function, the FN-DMC spin density closely resembles that obtained at the variational HF level. Similarly, when using various SOMO KS orbitals obtained with a variable exchange hybrid (B3LYP) DFT method, FN-DMC spin densities resembling their KS counterparts are obtained. As a consequence, it becomes impossible to decide on such grounds what is the correct chemical picture for the spin distribution. Nevertheless, we have noted that, within the framework of FN-DMC approaches there exists an internal criterion allowing to estimate the nodal quality: The lower the fixed-node energy is, the "better" the nodes are expected to be (variational property of the fixed-node energy; see ref 21). We recall that this criterion should be taken with lot of caution for a property other than the energy; however, it is worth noting that the nodes of the SOMO minimizing the fixed-node energy are those corresponding to a contribution of HF exchange of about 40−45%, considerably larger than ordinary B3LYP but much smaller than pure HF.

In order to elucidate these various contradictory results, we have performed near-Full Configuration Interaction calculations. Only such calculations can indeed yield a reliable balance between electron correlation and exchange effects. In the


dx.doi.org/10.1021/ct5004252 | J. Chem. Theory Comput. XXXX, XXX, XXX−XXX

present case where the molecule contains 63 electrons, ordinary FCI calculations using standard basis sets are just unfeasible. To circumvent this difficulty we have proposed (i) to employ the small 6-31G basis set and (ii) to make use of a perturbatively selected CI (CIPSI) approach to avoid the huge intractable FCI expansions, even for this small basis set (about $10^{18}$ determinants in the FCI space). Clearly, by using a small basis set only semiquantitative results can be obtained. However, since all types of electronic excitations are considered,[36] it can be expected that such calculations can give some useful information on the origin of the conflicting results among various approaches. Quite remarkably, it turns out that the FCI/6-31G results are in this respect particularly illuminating (see in Section 6, the dependence of the energy gap and of the spin density as a function of the number of determinants and on the nature of the orbitals). It is unlikely that such important aspects will be qualitatively changed when using larger basis sets in the FCI calculation.

From the set of data obtained for total energies, energy gap, spin densities, and the dependence of the various results on the number of determinants and types of molecular orbitals used, a rather coherent chemical picture emerges. At the uncorrelated (SCF) level, the lowest state is of $^2\sum_g^+$ symmetry and the Cu(3d) hole is completely localized on the copper atom. When dynamical correlation effects are added the ordering between the $^2\sum_g$ and $^2\Pi_g$ states is reversed and the hole is found to partly delocalize over the Cl ligands. At the ordinary DFT-B3LYP level, the Cu(3d) hole is too much delocalized over the chlorine atoms due to an improper balance between the self-interaction and exchange effects. To get a chemically meaningful description of electronic distributions using B3LYP-DFT, the percentage of HF exchange used must be increased up to about 40%. At the fixed-node DMC level, spin densities are found to be intimately related to the shape of the singly occupied molecular orbital, an orbital whose nodes are in turn directly related to the level of HF exchange used to derive it. Using as criterion the minimization of the FN-DMC ground-state energy, the optimal nodes for the SOMO are obtained for a HF exchange weight of about 40%, a result coherent with what has been obtained with near-FCI. Finally, let us note that the fact that DFT overestimates delocalization effects of magnetic holes in molecular systems has already been noticed in the literature by other authors (see, e.g., ref 37).

## AUTHOR INFORMATION


### Corresponding Author

*E-mail: caffarel@irsamc.ups-tlse.fr.

### Present Address

[†]On sabbatical leave from Facultad de Ciencias, Universidad Autónoma del Estado de Morelos, Morelos, CP 62209, Mexico.


### Notes

The authors declare no competing financial interest.

## ACKNOWLEDGMENTS

We acknowledge a fruitful discussion with Jeremy Harvey about the role of the exchange in metal-containing molecular systems. The Agence Nationale pour la Recherche (ANR) is thanked for support through Grant No ANR 2011 BS08 004 01. A.R.S. thanks support from CONACYT (Mexico) sabbatical program and from the Professeur Invité program from the Université de Toulouse. This work has been made possible through generous computational support from CALMIP (Toulouse) under the allocation 2013-0510 and GENCI under the allocation x2014081738.

## REFERENCES


(1) Wagner, L. *Chem. Phys. Lett.* **2003**, *370*, 412.
(2) Wagner, L.; Mitas, L. *J. Chem. Phys.* **2007**, *126*, 034105.
(3) Wagner, L. *J. Phys: Condens. Matter* **2007**, *19*, 343201.
(4) Kolorenč, J.; Hu, S.; Mitas, L. *Phys. Rev. B* **2010**, *82*, 115108.
(5) Ross, A.; Crozet, P.; Bacis, R.; Churassy, S.; Erba, B.; Ashworth, S.; Lakin, N.; Wickham, M.; Beattie, I.; Brown, J. *J. Mol. Spectrosc.* **1996**, *177*, 134.
(6) Bouvier, A.; Bosch, E.; Bouvier, A. *Chem. Phys.* **1996**, *202*, 139.
(7) Bosch, E.; Crozet, P.; Roos, A.; Brown, J. *J. Mol. Spectrosc.* **2000**, *202*, 253 and references therein..
(8) Lorenz, M.; Caspary, N.; Foeller, W.; Agreiter, J.; Smith, A.; Bondibey, V. *Mol. Phys.* **1997**, *91*, 483.
(9) Lorenz, M.; Smith, A.; Bondibey, V. *J. Chem. Phys.* **2002**, *115*, 8251.
(10) Ramírez-Solís, A.; Daudey, J. *J. Chem. Phys.* **2004**, *120*, 3221.
(11) Ramírez-Solís, A.; Daudey, J. *J. Chem. Phys.* **2005**, *122*, 14135.
(12) Bauschlicher, C.; Roos, B. *J. Chem. Phys.* **1989**, *91*, 4785.
(13) Ramírez-Solís, A.; Poteau, R.; Vela, A.; Daudey, J. *J. Chem. Phys.* **2005**, *122*, 164306.
(14) Using 21 active electrons (11 from Cu and 5 from each Cl atom) in the 3p orbitals of both Cl and 3d,4s,4p of Cu, a CASSCF(21,15) is defined. However, at the time of the original works[10,11,13] one active orbital was removed because of computational restrictions (ACPF not feasible) and a CASSCF(21,14) wave function was thus considered as reference for the benchmark ACPF calculations. In practice, the difference between the CASSCF(21,14) and CASSCF(21,15) wave functions is negligible. However, for the sake of coherence (comparison between old and present results) an active space built using 14 orbitals has been kept here.
(15) Pou-Amerigo, R.; Merchan, M.; Nebot-Gil, I.; Widmark, P.; Roos, B. *Theor. Chim. Acta* **1995**, *92*, 149.
(16) Widmark, P.; Persson, B. J.; Roos, B. *Theor. Chim. Acta* **1991**, *79*, 419.
(17) Assaraf, R.; Caffarel, M.; Khelif, A. *Phys. Rev. E* **2000**, *61*, 4566.
(18) Caffarel, M. Quantum Monte Carlo Methods in Chemistry. In *Encyclopedia of Applied and Computational Mathematics*; Bjorn Engquist, S., Ed.; Springer: New York, 2012; Vol. *1*.
(19) Caffarel, M.; Claverie, P. *J. Chem. Phys.* **1988**, *88*, 1088.
(20) Baroni, S.; Moroni, S. *Phys. Rev. Lett.* **1999**, *82*, 4745.
(21) Hammond, B.; Lester, W. A., Jr.; Reynolds, P. In *Monte Carlo Methods in Ab Initio Quantum Chemistry*; World Scientific Lecture and Course Notes in Chemistry; World Scientific: Singapore, 1994; Vol. *1*.
(22) Davidson, E.; Hagstrom, S.; Chakravorty, S.; Umar, V. M.; Fischer, C. F. *Phys. Rev. A* **1993**, *47*, 3649.
(23) Bunge, C.; Barrientos, J.; Bunge, A.; Cogordan, J. *Phys. Rev. A* **1992**, *46*, 3691.
(24) Clementi, E.; Hofmann, D. *J. Mol. Struct.: THEOCHEM* **1995**, *330*, 17.
(25) Weigend, F.; Ahlrichs, R. *Phys. Chem. Chem. Phys.* **2005**, *7*, 3297.
(26) Huron, B.; Rancurel, P.; Malrieu, J. *J. Chem. Phys.* **1973**, *58*, 5745.
(27) Evangelisti, S.; Daudey, J.; Malrieu, J. *J. Chem. Phys.* **1983**, *75*, 91.
(28) Giner, E.; Scemama, A.; Caffarel, M. *Can. J. Chem.* **2013**, *91*, 879.
(29) Ramírez-Solís, A.; Daudey, J. *Chem. Phys.* **1989**, *134*, 111.
(30) Ramírez-Solís, A.; Daudey, J. *J. Phys. B* **1990**, *23*, 2277.
(31) Ramírez-Solís, A.; Daudey, J. *Phys. Rev. A* **1990**, *42*, 5168.
(32) Ramírez-Solís, A.; Daudey, J.; Teichteil, C. *J. Chem. Phys.* **1990**, *93*, 7277.
(33) Ramírez-Solís, A.; Schamps, J. *J. Chem. Phys.* **1995**, *102*, 4482.
(34) Ramírez-Solís, A.; Daudey, J. *J. Chem. Phys.* **2000**, *113*, 8580.
(35) Ramírez-Solís, A.; Ruiz, M.; Novaro, O.; Daudey, J. *Z. Phys. D: At., Mol. Clusters* **1990**, *15*, 71.

(36) In practice, excitations up to quintuples are treated variationally, those up to septuples perturbatively, the others having a negligible contribution.
(37) Cabrero, J.; Calzado, C.; Maynau, D.; Caballol, R.; Malrieu, J. *J. Phys.Chem. A* **2002**, *106*, 8146.